Molecular Simulation of the Potential of Methane Reoccupation during the Replacement of Methane Hydrate by CO_2

Chun-Yu Geng,[†,‡] Hao Wen,[*,†] and Han Zhou[§]

State Key Laboratory of Multi-Phase Complex Systems, Institute of Process Engineering, Chinese Academy of Sciences, No. 1 2nd North Lane, ZhongGuanCun, Beijing 100190, China, Graduate University of Chinese Academy of Sciences, P.O. Box 4588, Beijing 100049, China, and Research Institute of Petroleum Processing, SINOPEC, No.18 Xueyuan Road, Beijing 100083, China

Received: December 29, 2008; Revised Manuscript Received: March 23, 2009

Molecular dynamics simulations and stabilization energy calculations are performed in this work in order to understand the stability of CH_4 hydrate, CO_2 hydrate, and CH_4-CO_2 mixed hydrate. The model systems of fully occupied type SI CH_4 hydrate, CO_2 hydrate, and CH_4-CO_2 mixed hydrate are prepared in a simulation box of $2 \times 2 \times 2$ unit cell with periodic boundary conditions. The MD simulation results reveal that the CH_4-CO_2 mixed hydrate is the most stable one in above three hydrates. The stabilization energy calculations of small and large cavities occupied by CH_4 and CO_2 show that the CO_2 molecule is less suitable for the small cavity because of its larger size compared with the CH_4 molecule but is more suitable for the large cavity. The results in this work can also explain the possibility of CH_4 molecule in reoccupying the small cavity during the replacement of CH_4 hydrate by CO_2, from the hydrate stability point of view.

1. Introduction

Natural gas hydrate (NGH) is expected to be a future energy resource, since the amount of NGH below the ocean floor is more than all of the current fossil fuel sources combined.[1] Methods based on decomposition of hydrate by external stimulations, such as thermal treatment, depressurizing, and adding inhibitors into the hydrate, have been proposed for producing natural gas from NGH.[2] Some researchers have also suggested that the decomposition of NGH could lead to weakening of the ocean floor.[3]

On the other hand, as the increasing anthropogenic carbon dioxide emission contributes to global warming, CO_2 hydrate is becoming a promising form for CO_2 storage that may help to the climate change mitigation.[4] Interest in CO_2 hydrate has intensified because of discussions on the possible disposal of isolating CO_2 from the atmosphere in deep oceans as a means of greenhouse gas emission reduction.[5–7] Therefore, replacement of natural gas from NGH by CO_2 is also a candidate for producing natural gas from NGH and disposal of CO_2.[8] This process is a favorable way as a long-term storage of CO_2 and enables the ocean floor to remain stable even after recovering the natural gas, because of the same structure of CH_4 and CO_2 hydrates.[9]

The possibility of replacing natural gas by CO_2 from NGH has been investigated. Measurements of three-phase (vapor−liquid−hydrate) equilibria for $CO_2-CH_4-H_2O$ ternary system show that CO_2 hydrate is thermodynamically more stable than CH_4 hydrate below 283 K, since the equilibrium pressure of CO_2 hydrate is lower than that of CH_4 hydrate.[10–12] Further, the Gibbs free energy of the replacement is found to be a negative value from molecular simulation.[13] This thermodynamic evidence supports the replacement in hydrate at appropriate conditions.

Typically, both CH_4 and CO_2 can form hydrates of type structure I (SI) crystallographic structure,[14,15] in which the small cavity is composed of 12 pentagonal faces (a dodecahedral framework) of 20 H_2O molecules and forms a dodecahedron framework, and the large one is composed of 12 pentagonal faces and two hexagonal faces of 24 H_2O molecules and forms a tetrakaidecahedron framework. Though measurements using Raman spectroscopy of SI CO_2 hydrate do not show any splitting in the Raman frequencies, buttressing the notion that CO_2 molecules occupy only large cavities,[16] infrared spectra of the double clathrate, such as carbon dioxide−ethylene oxide, suggest that the CO_2 molecules can occupy both the dodecahedron and the tetrakaidecahedron cavities.[17,18] Crystal structure of type SI CO_2 hydrate has been carried out to confirm that CO_2 molecules can occupy both the small and large cavities.[18] Ota et al.[19] presented an experimental study on the replacement of CH_4 in hydrate with liquid CO_2 and used a view cell for visual observation and Raman spectroscopy for analysis. They found that the CH_4 molecules released from hydrate could reoccupy the small cavities.

In this work, the structures and stability of type SI CH_4 and CO_2 hydrates are studied using molecular dynamics (MD) simulations. Previously, Ding et al.[20] have investigated the partly and fully occupied hydrates and observed a similar dissociation behavior except for the stability for the different occupancy of the hydrates; therefore, the fully occupied hydrates can be used in our simulations to avoid influence of the hydrate occupancy. For understanding the potential of CH_4 molecules in reoccupying the small cavities, the stabilities of CH_4 hydrate and CO_2 hydrate at different temperatures are compared with that of the CH_4-CO_2 mixed hydrate where CH_4 molecules are encaged in small cavities and CO_2 molecules in large cavities. The tendency of small cavity reoccupation can also be understood by comparison of the stabilization energies of the small and large cavities occupied by CH_4 and CO_2.

* To whom correspondence should be addressed. E-mail: hwen@home.ipe.ac.cn.
† Institute of Process Engineering.
‡ Graduate University of Chinese Academy of Sciences.
§ Research Institute of Petroleum Processing.

10.1021/jp811474m CCC: $40.75
Published on Web 04/10/2009

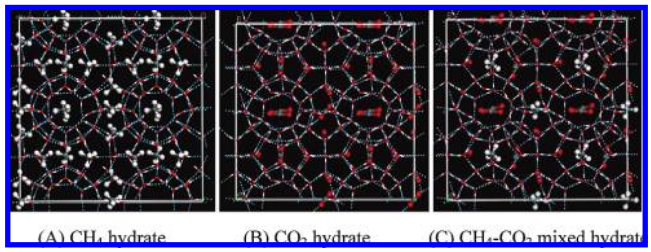

Figure 1. Iinitial configurations of model systems of fully occupied type SI gas hydrates: red for O atoms; light-gray for H atoms; dark-gray for C atoms; light-blue dashed lines for the hydrogen bonding network between H_2O molecules.

2. Simulation Details

2.1. Simulation Systems and Simulation Methods. The model systems prepared in this work are fully occupied type SI CH_4 hydrate, CO_2 hydrate, and CH_4-CO_2 mixed hydrate in a simulation box of $2 \times 2 \times 2$ unit cell with periodic boundary conditions, as shown in Figure 1. The model system of CH_4 hydrate consists of 64 CH_4 molecules and 368 H_2O molecules, while CO_2 hydrate consists of 64 CO_2 and 368 H_2O molecules. The CH_4-CO_2 mixed hydrate consists of 16 CH_4, 48 CO_2, and 368 H_2O molecules, with CH_4 molecules encaged in small cavities and CO_2 molecules in large cavities. The initial positions of H_2O molecules in model systems are taken from X-ray diffraction measurements,[21,22] where the gas (CH_4 or CO_2) molecules are encaged in the center of cavities. Additionally, all atomic positions are allowed to freely translate during the simulation.

The *NPT* ensemble molecular dynamics (MD) simulations are performed with CVFF force field at pressure $P = 50$ bar and temperatures $T = 260$, 270, and 280 K, using the Materials Studio software.[23] The temperature and pressure of the model systems are controlled using Andersen[24] and Berendsen[25] methods, respectively. The initial equilibrations of the model systems are optimized by both steepest descent and conjugate gradient. The van der Waals and long-range Coulomb interactions are calculated with the Ewald summation. The Verlet velocity algorithm[26] is used to obtain accurate integrations and statistical ensembles.

Simulation time of 200 ps with an integration time step of 1 fs is typically employed at each temperature, and simulations of the first 50 ps are used for equilibration. The position and orientation of H_2O molecules are fixed in the first 5 ps simulations during the energy optimization in order to make sufficient movements of the gas molecules. All simulations are performed on the server with Intel Xeon CPU E5335 2.0 GHz and 4G memories.

2.2. Stabilization Energy of Small and Large Cavities. Structures of the small and large cavities in type SI hydrate from single crystal X-ray diffraction[21,22] are shown in Figure 2. The small cavity is a dodecahedral framework constructed by 20 H_2O molecules represented as (5^{12}), while the large cavity is a tetrakaidecahedral framework constructed by 24 H_2O molecules as $(5^{12}6^2)$. The gas molecule occupied cavities are constructed by placing the CH_4 or CO_2 molecule at the center of small and large cavities according to Udachin and IDA et al.'s results,[18,27] represented as $CH_4\cdot(5^{12})$, $CO_2\cdot(5^{12})$, $CH_4\cdot(5^{12}6^2)$, and $CO_2\cdot(5^{12}6^2)$ in this work for simplification.

The structure optimization of cavities occupied by gas molecules is performed using the hybrid density functional theory in order to compare the stabilization energies of cavities occupied by CH_4 and CO_2. The hybrid density functional theory

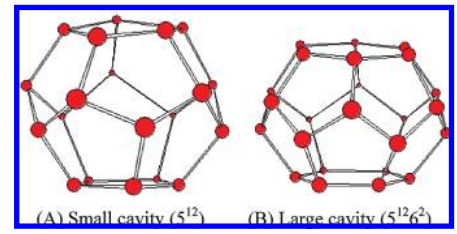

Figure 2. Schematic framework of H_2O molecule cavities in type SI gas hydrates.

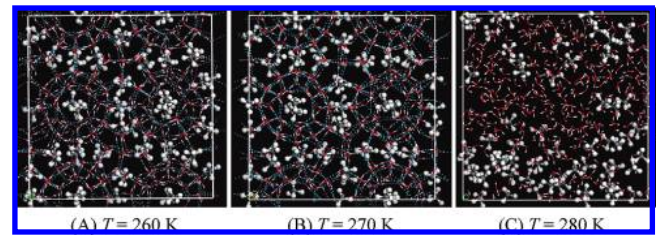

Figure 3. Snapshots of the final configurations of CH_4 hydrate at 260, 270, and 280 K.

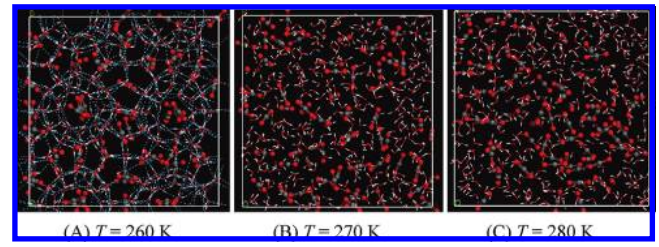

Figure 4. Snapshots of the final configurations of CO_2 hydrate at 260, 270, and 280 K.

used in this work is Becke's three-parameter hybrid functional[28] with Lee, Yang, and Parr's correlation functional (B3LYP),[29] using the 6-31g(d,p) basis set. According to ref 30, the stabilization energy of a cavity occupied by a gas molecule is defined as the difference between the total energy of cavities occupied by gas molecules and those of separated H_2O and gas molecules involved in the cavity occupied by a gas molecule. Thus, in this work, the stabilization energy of cavity occupied by a gas molecule ΔE_{GH} can be calculated by

$$\Delta E_{GH} = E_{GH\text{-cavity}} - \sum_i (E_{H_2O})_i - E_{gas} \quad (1)$$

where $E_{GH\text{-cavity}}$ is the total energy of cavity occupied by gas molecule, E_{H_2O} and E_{gas} are the energies of H_2O and gas molecules involved in the cavity occupied by the gas molecule, respectively.

The aforementioned calculations are performed by using the Gaussian 03 program[31] on the Shenteng 6800 workstation provided by the Computer Network Information Center, Chinese Academy of Sciences.

3. Results and Discussion

3.1. Snapshots of the Final Configurations. Snapshots of the final configurations of CH_4 hydrate, CO_2 hydrate, and CH_4-CO_2 mixed hydrate at pressure $P = 50$ bar and temperatures $T = 260$, 270, and 280 K are presented in Figures 3−5. Figures 3 and 5 indicate that the crystal structure of CH_4 hydrate and CH_4-CO_2 mixed hydrate can keep stable at 270 K; even

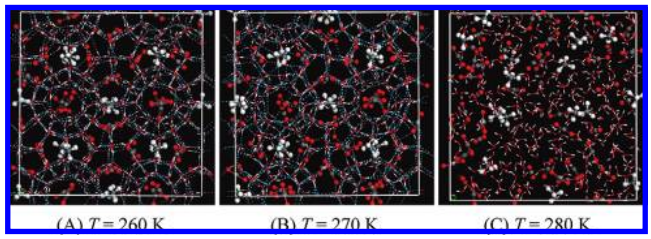

Figure 5. Snapshots of the final configurations of CH_4-CO_2 mixed hydrate at 260, 270, and 280 K.

distortions of the hydrogen bonding network between H_2O molecules appeared. An evident collapse of the hydrogen bonding network in CO_2 hydrate can be observed at 270 K as presented in Figure 4; however, no aggregation of CO_2 molecules observed. When the system temperature grows to 280 K, observable aggregation of CH_4 and CO_2 molecules appears in decomposed CH_4 and CO_2 hydrates. Moreover, the CH_4 molecules exhibit higher aggregation tendency than CO_2 molecules do. While in the CH_4-CO_2 mixed hydrate, although there are some guest molecules clustering at 280 K, most of the CH_4 and CO_2 molecules are still dispersed in water. Additionally, the average energies of CH_4 hydrate, CO_2 hydrate, and CH_4-CO_2 mixed hydrate at 280 K are −1952.0, −2456.5, and −2549.4 kcal·mol^{-1}, respectively. The result indicates that CH_4-CO_2 mixed hydrate could be more stable than CH_4 or CO_2 hydrate at the same temperature and pressure.

3.2. Radial Distribution Function (RDF). The radial distribution functions (RDFs) of O and C atoms at $P = 50$ bar and $T = 260$, 270, and 280 K for CH_4 hydrate, CO_2 hydrate, and CH_4-CO_2 mixed hydrate are presented in Figures 6 and 7.

In Figure 6, the RDFs of O atom g_{OO} in H_2O molecules, for CH_4 hydrate, CO_2 hydrate, and CH_4-CO_2 mixed hydrate, display a structural consistency with the recent simulations.[32,33] The maximal RDF peaks of the O atom in H_2O molecules appear at a distance of $r_{OO} = 2.78$ Å, corresponding to the nearest distance between H_2O molecules separated from each other at around 2.78 Å. The second maximal peaks appeared at $r_{OO} = 4.53$ Å and indicate the existence of tetrahedral hydrogen bonding structures of H_2O molecules in gas hydrates.[20] In Figure 7, the RDF peaks of C atoms in CH_4 and/or CO_2 molecules g_{CC} appear at $r_{CC} = 6.7$ Å with excellent agreement with the recent neutron diffraction results and pair correlation functions for gas hydrate.[34] The RDF peaks of C atoms appear at $r_{CC} = 4.1$ Å and show that the dissociation of hydrates with aggregation of gas molecules occurred when the system temperature rises to 280 K.

It can be seen from Figures 6 and 7 that the gradually lower and broader g_{OO} peaks at 2.78 and 4.53 Å and g_{CC} peaks at 6.7 Å with rising temperature indicate the hydrates becoming less stable, while the appearance and growth of g_{CC} peaks at approximately 4.1 Å imply the aggregation of CH_4 and/or CO_2 molecules. The g_{OO} and g_{CC} peaks appearing in CH_4-CO_2 mixed hydrate are slightly higher than those in CH_4 and CO_2 hydrates at the same temperature and pressure, indicating the higher stability of CH_4-CO_2 mixed hydrate.

The RDFs of O atom for CH_4 hydrate, CO_2 hydrate, and CH_4-CO_2 mixed hydrate at $P = 50$ bar and $T = 280$ K are presented in Figures 8 and those of the C atom in Figure 9 for further comparison of the stability of different gas hydrates. For RDF peaks of O atoms and those of C atoms at $r_{CC} = 6.7$ Å, the sharper peak represents the higher hydrate stability while the RDF peaks of C atoms at $r_{CC} = 4.1$ Å are opposite. The

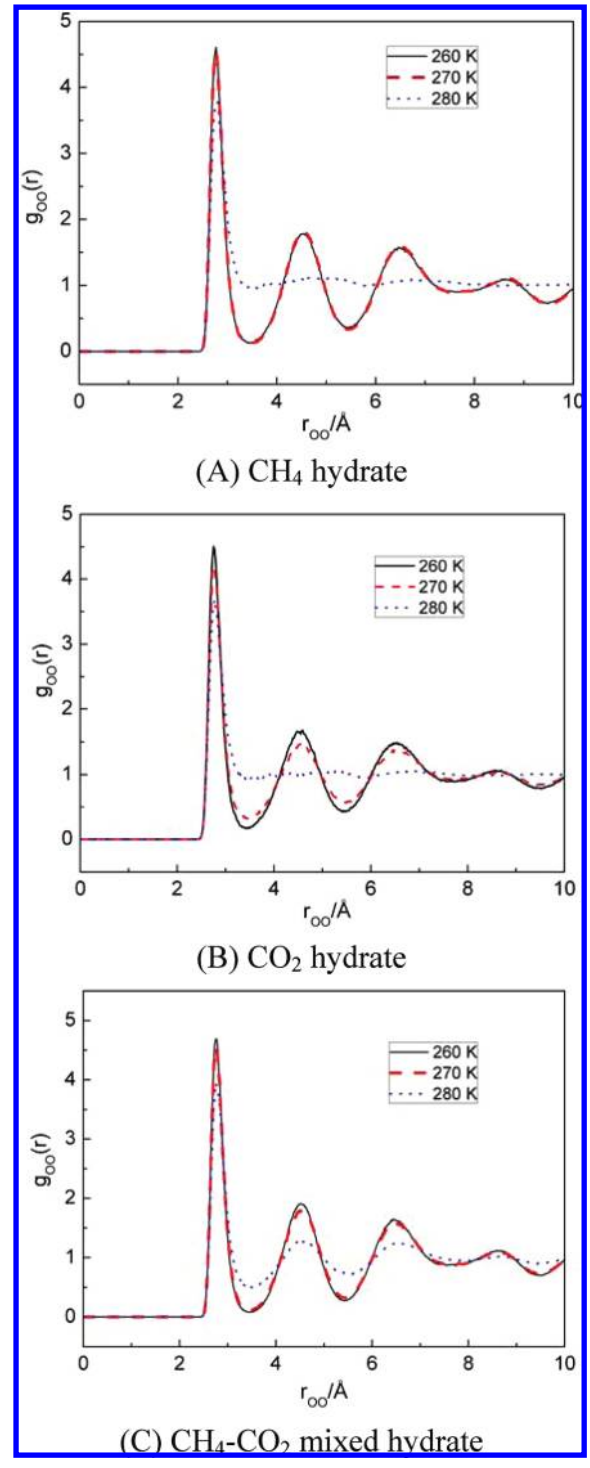

Figure 6. RDFs of O atom in H_2O molecules at 50 bar and 260, 270, and 280 K for (A) CH_4 hydrate, (B) CO_2 hydrate, and (C) CH_4-CO_2 mixed hydrate.

CH_4-CO_2 mixed hydrate exhibits higher stability compared with the CH_4 hydrate and CO_2 hydrate. Although the crystal structure of the CH_4-CO_2 mixed hydrate decomposes at 280 K, the occurrence of gas-molecule aggregation in the CH_4-CO_2 mixed hydrate is evidently less than those in CH_4 hydrate and CO_2 hydrate, which can be observed as different by the higher RDF peak of C atoms at 6.7 Å and lower peak at 4.1 Å.

3.3. Mean Square Displacement (MSD). The mean square displacement (MSD) is a measure of the average distance a

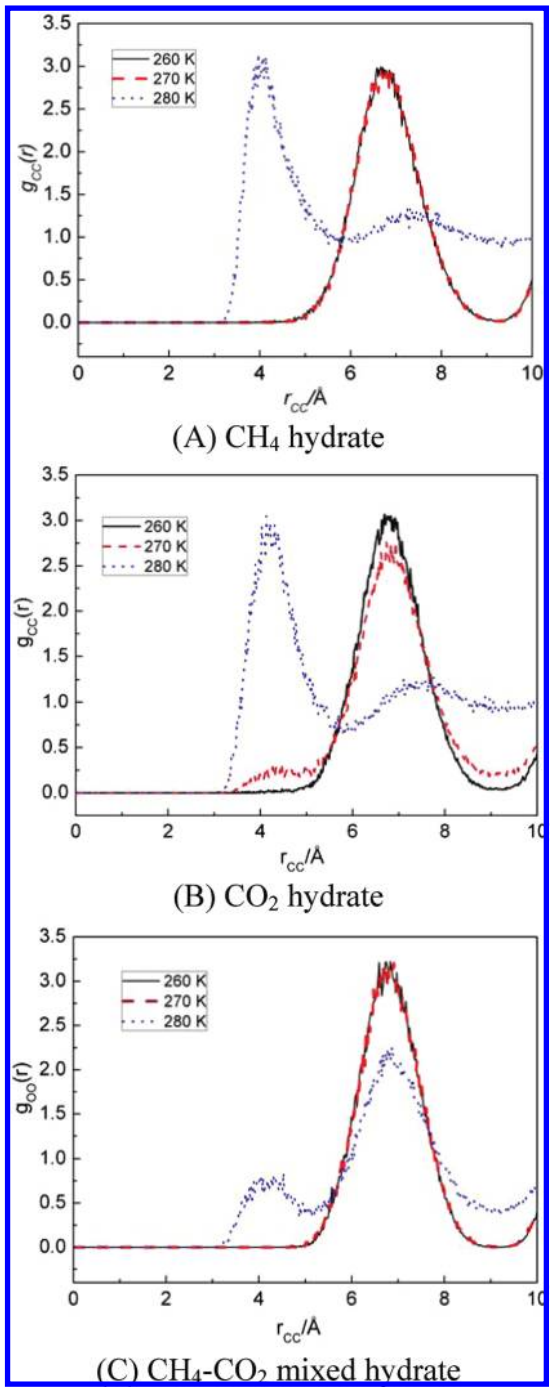

Figure 7. RDFs of C atom in CH_4 and/or CO_2 molecules at 50 bar and 260, 270, and 280 K for (A) CH_4 hydrate, (B) CO_2 hydrate, and (C) CH_4-CO_2 mixed hydrate.

molecule travels. For a stable crystal, the constituent molecules vibrate around their lattice sites without diffusing.

Figures 10−12 illustrate the MSD profiles of H_2O molecules in the CH_4 hydrate, CO_2 hydrate, and CH_4-CO_2 mixed hydrate at $P = 50$ bar and $T = 260$, 270, and 280 K. In Figure 11, it indicates that H_2O molecules in CO_2 hydrate is slightly diffusing at 270 K, while those in CH_4 hydrate and in CH_4-CO_2 mixed hydrate still show a typical feature of crystalline solid until the temperature approaches 280 K, as shown in Figures 10 and 12. The collapse of the crystal structure and H_2O molecule diffusion occurs in the three hydrates when temperature approaches 280 K.

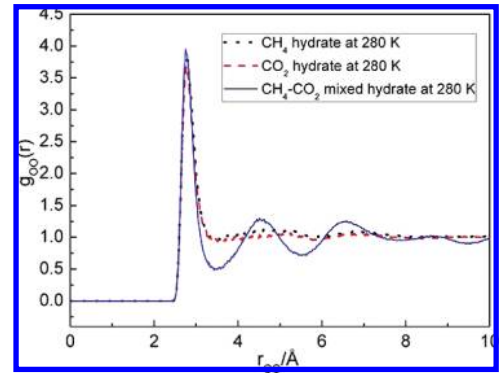

Figure 8. RDFs of O atom in H_2O molecules for CH_4 hydrate, CO_2 hydrate, and CH_4-CO_2 mixed hydrate at 50 bar and 280 K.

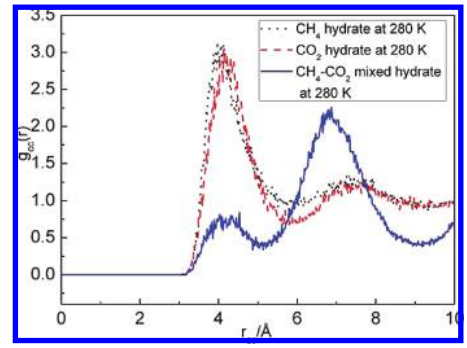

Figure 9. RDFs of C atoms in CH_4 and/or CO_2 molecules for CH_4 hydrate, CO_2 hydrate, and CH_4-CO_2 mixed hydrate at 50 bar and 280 K.

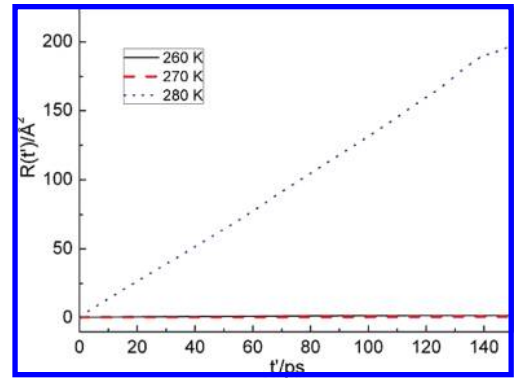

Figure 10. MSD of H_2O molecules in CH_4 hydrate at 50 bar and 260, 270, and 280 K.

A comparison of MSD of H_2O molecules in the CH_4 hydrate, CO_2 hydrate, and CH_4-CO_2 mixed hydrate at 270 and 280 K is shown in Figure 13. H_2O molecules show an obviously larger MSD value in the CO_2 hydrate than those in CH_4 hydrate and in CH_4-CO_2 mixed hydrate at 270 K. This predicted larger MSD is indicative of partial decomposition of CO_2 hydrate at 270 K. In addition, H_2O molecules in CH_4 hydrate show larger MSD values than those in CH_4-CO_2 mixed hydrate do at 280 K, implying that the diffusion of CH_4 hydrate is obviously stronger than the CH_4-CO_2 mixed hydrate. Accordingly, the decomposition of CH_4 hydrate is much more pronounced than the CH_4-CO_2 mixed hydrate at 280 K.

Figure 14 presents the predicted diffusion coefficients of CH_4 in the CH_4 hydrate and the CH_4-CO_2 mixed hydrate and those of CO_2 in CO_2 hydrate and CH_4-CO_2 mixed hydrate at 260, 270, and 280 K. A comparison of the predicted diffusion coefficients of CH_4 and CO_2 in different hydrates indicates that a significant diffusive motion of the CO_2 hydrate can be

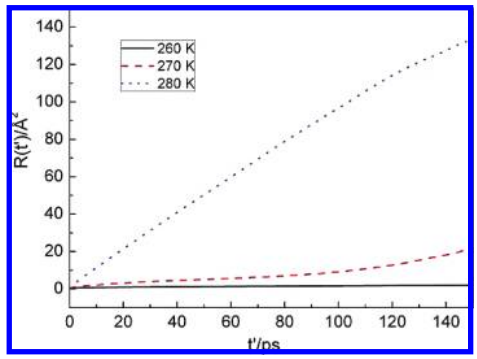

Figure 11. MSD of H_2O molecules in CO_2 hydrate at 50 bar and 260, 270, and 280 K.

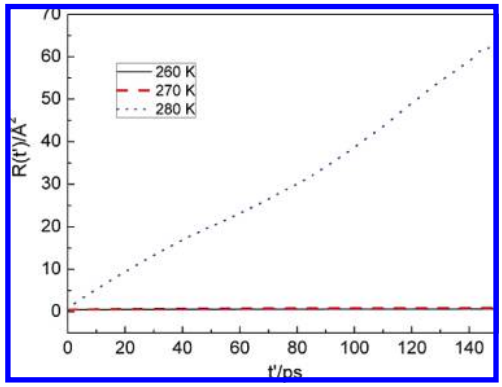

Figure 12. MSD of H_2O molecules in CH_4-CO_2 mixed hydrate at 50 bar and 260, 270, and 280 K.

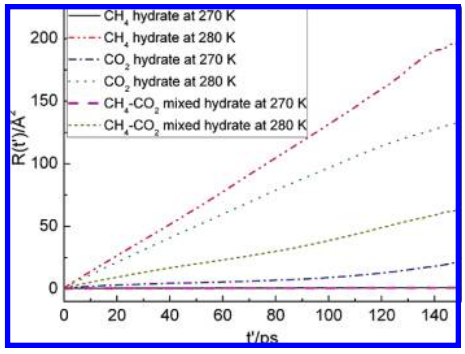

Figure 13. MSD of H_2O molecules in CH_4 hydrate, CO_2 hydrate, and CH_4-CO_2 mixed hydrate at 270 and 280 K.

observed at 270 K. However, the calculations predict that CH_4 molecules evidently become more diffusive in the CH_4 hydrate at 280 K. Furthermore, at the same temperature, the diffusion is less efficient in the CH_4-CO_2 hydrate than in the other hydrates. Additionally, the diffusion coefficient of CO_2 hydrate at 273 K in Demurov's result[35] in which 70% of the small cavities are occupied by CO_2 molecules is much lower than that of our fully occupied CO_2 hydrate at 270 K, and it is obviously higher than that of the CH_4-CO_2 mixed hydrate. The prediction of less efficient diffusion in the mixed hydrate implies that the decomposition of this phase is weaker than either of the others. The result obtained agrees with RDF, which also indicates that the CH_4-CO_2 mixed hydrate is the most stable hydrate of the three.

3.4. Stabilization Energies. Calculations and comparisons on the stabilization energies of CH_4 and CO_2 occupying small and large cavities are performed in an attempt to comprehend the stability of the CH_4 hydrate, the CO_2 hydrate, and the CH_4-CO_2 mixed hydrate. The small and large cavities of the

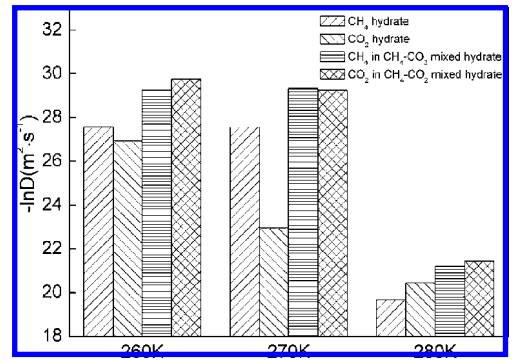

Figure 14. Diffusion coefficients of CH_4 and CO_2 molecules in CH_4 hydrate, CO_2 hydrate, and CH_4-CO_2 mixed hydrate at 260, 270, and 280 K.

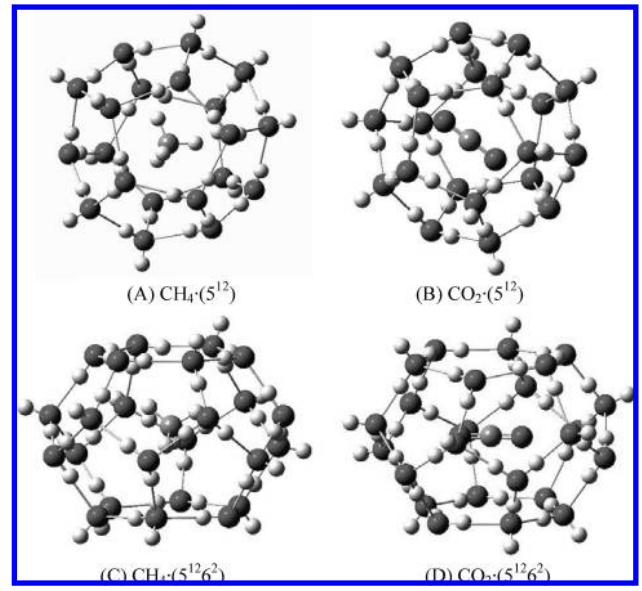

Figure 15. Optimized structures of small and large cavities occupied by CH_4 and CO_2.

hydrate structure from single-crystal X-ray diffraction[21,22] are used as the initial structures for energy optimization. The optimized cavity structures are shown in Figure 15.

For $CH_4\cdot(5^{12})$ and $CO_2\cdot(5^{12})$, there are 30 hydrogen-bonding H atoms in each small cavity with average O−H bond length of ∼0.99 Å. The average H−O−H bond angle of H_2O molecule is ∼106°. The O−O distance in the dodecahedral structure is 2.73 Å, and the O−O−O angle ∼108°. The O−H···O angle is ∼176°, and the average bond length of H···O hydrogen bond is 1.75 Å, which represents an effective hydrogen bond. The stabilization energy of $CH_4\cdot(5^{12})$ is −292.2 kcal·mol^{-1}, and that of $CO_2\cdot(5^{12})$ −285.3 kcal·mol^{-1}.

For $CH_4\cdot(5^{12}6^2)$ and $CO_2\cdot(5^{12}6^2)$, both of the two cavities have an average O−O distance of ∼2.72 Å and O−O−O angle of 110°. There are 36 hydrogen-bonding H atoms in each large cavity. Similarly, the average hydrogen bonding O−H bond length and H−O−H angle of the H_2O molecule in the large cavity are 0.99 Å and 106°, respectively. The H···O hydrogen bond is ∼1.73 Å, and the O−H···O angle 176°. The stabilization energy of $CH_4\cdot(5^{12}6^2)$ is −357.1 kcal·mol^{-1}, and that of $CO_2\cdot(5^{12}6^2)$ −369.0 kcal·mol^{-1}.

The structural parameters of cavities occupied by CH_4 or CO_2 indicate that the gas hydrate cavities do not distort the hydrogen-bonding network, and the size of either small or large cavity is big enough to accommodate a CH_4 or a CO_2 molecule. For

TABLE 1: Stabilization Energies of Different Clusters[a]

cluster	$E_{GH\text{-}cavity}$, hartree	ΔE_{GH}, hartree	ΔE_{GH}, kcal·mol^{-1}
$CH_4\cdot(5^{12})$	−1569.3537	−0.4657	−292.2
$CO_2\cdot(5^{12})$	−1717.3996	−0.4546	−285.3
$CH_4\cdot(5^{12}6^2)$	−1875.1299	−0.5691	−357.1
$CO_2\cdot(5^{12}6^2)$	−2023.2058	−0.5880	−369.0

[a] The energies of optimized structures for H_2O, CH_4, and CO_2 molecules are −76.4182, −40.5240, and −188.5810 hartree, respectively.

comparison of the stability of cavities occupied by CH_4 and CO_2, the stabilization energies of $CH_4\cdot(5^{12})$, $CO_2\cdot(5^{12})$, $CH_4\cdot(5^{12}6^2)$, and $CO_2\cdot(5^{12}6^2)$ are calculated in accordance to eq 1, as presented in Table 1. The calculated stabilization energy of $CH_4\cdot(5^{12})$ is somewhat larger than Khan's[30] HF and MP2 results, which should be attributed to the different method (B3LYP) used in our calculations. A comparison of the stabilization energy of $CH_4\cdot(5^{12})$, $CO_2\cdot(5^{12})$, $CH_4\cdot(5^{12}6^2)$, and $CO_2\cdot(5^{12}6^2)$, where the CH_4 and CO_2 molecules are encaged in the small and large cavities, respectively, suggests that $CO_2\cdot(5^{12})$ is less stable than $CH_4\cdot(5^{12})$ in the small cavity while $CO_2\cdot(5^{12}6^2)$ is more stable than $CH_4\cdot(5^{12}6^2)$ in the large cavity.

Ota et al.[19] reported that during the replacement of CH_4 in the hydrate by use of CO_2, the decomposition of the large cavity in the CH_4 hydrate proceeded more quickly than that of the small cavity and some portions of the released CH_4 molecules reoccupied the small cavity because the CO_2 molecule is too large to be encaged in the small cavity. Given that CO_2 is somewhat larger than CH_4, the CO_2-H_2O interaction potential in the small cavity should be more repulsive in nature, as seen from the stabilization energies of $CH_4\cdot(5^{12})$ and $CO_2\cdot(5^{12})$ that we have calculated. The difference in stabilization energies, as seen from a comparison of the stabilization energies of $CH_4\cdot(5^{12}6^2)$ and $CO_2\cdot(5^{12}6^2)$, also suggests that the CO_2 molecule is more suited than the CH_4 molecule to be accommodated in the large cavity. The stabilization energy calculations also support the consideration from MD simulations that the CH_4-CO_2 mixed hydrate is the most stable of the three hydrates of CH_4, CO_2, and CH_4-CO_2 mixed. Therefore, during the replacement of CH_4 in the hydrate by CO_2, it is easier to form the CH_4-CO_2 mixed hydrate because of its stability.

4. Conclusions

The stabilities of the fully occupied type SI CH_4 hydrate, the CO_2 hydrate, and the CH_4-CO_2 mixed hydrate have been studied by molecular dynamics (MD) simulations at $P = 50$ bar and $T = 260$, 270, and 280 K. The final configurations, the radial distribution functions of the O atoms in the H_2O molecules and the C atoms in CH_4 and CO_2, the mean square displacements, and the calculated diffusion coefficients of H_2O, CO_2, and CH_4 in the various hydrates all indicate that the CH_4-CO_2 mixed hydrate is the most stable of the three hydrates discussed. The calculation of the structures and the stabilization energies of CH_4 and CO_2 occupying small and large cavities indicate that cavities occupied by CH_4 or CO_2 do not distort the hydrogen-bonding network. A comparison of the stabilization energy indicates that $CO_2\cdot(5^{12})$ is less stable than $CH_4\cdot(5^{12})$, whereas $CO_2(5^{12}6^2)$ is fairly stable in comparison with $CH_4\cdot(5^{12}6^2)$.

A comparison of the stabilization energies of the small and large cavities containing CH_4 and CO_2 shows that the CO_2 molecule is less suitable for the small cavity than the CH_4 molecule but is more suitable for the large cavity. Combining the results from MD simulations with the stabilization energy calculations, one concludes that the CH_4-CO_2 mixed hydrate exhibits the best stability of the three hydrates considered in this work. In other words, it is possible to form the CH_4-CO_2 mixed hydrate during the replacement of CH_4 in the hydrate by CO_2. From the hydrate-stability point of view, the results of this work are consistent with the experimental study by Ota et al.[19] and can also account for the CH_4 reoccupation of the small cavity during the replacement of CH_4 hydrate by CO_2.

Acknowledgment. The authors gratefully appreciate the financial support from the National Natural Science Foundation of China (Grant No. 20821092). The authors also acknowledge generous computational services provided on the Shenteng 6800 workstation referred by the Computer Network Information Center, Chinese Academy of Sciences.

References and Notes

(1) Collett, T. S. *AAPG Bull.* **2002**, *86*, 1971.
(2) Holder, G. D.; Kamath, V. A.; Godbole, S. P. *Annu. Rev Energy* **1984**, *9*, 427.
(3) Gunn, D. A.; Nelder, L. M.; Rochelle, C. A.; Bateman, K.; Jackson, P. D.; Lovell, M. A.; Hobbs, P. R. N.; Long, D.; Rees, J. G.; Schultheiss, P.; Roberts, J.; Francis, T. *Terra Nova* **2002**, *14*, 443.
(4) Sloan, E. D. *Clathrate Hydrates of Natural Gases*, 2nd ed.; M. Dekker: New York, 1998.
(5) Herzog, H.; Golomb, D.; Zemba, S. *Environ. Prog.* **1991**, *10*, 64.
(6) Saji, A.; Yoshida, H.; Sakai, M.; Tanii, T.; Kamata, T.; Kitamura, H. *Energy Convers. Manage.* **1992**, *33*, 643.
(7) Nishikawa, N.; Morishita, M.; Uchiyama, M.; Yamaguchi, F.; Ohtsubo, K.; Kimuro, H.; Hiraoka, R. *Energy Convers. Manage.* **1992**, *33*, 651.
(8) Ohgaki, K.; Takano, K.; Moritoki, M. *Kagaku Kogaku Ronbunshu* **1994**, *20*, 121.
(9) Uchida, T.; Ikeda, I. Y.; Takeya, S.; Kamata, Y.; Ohmura, R.; Nagao, J.; Zatsepina, O. Y.; Buffett, B. A. *ChemPhysChem* **2005**, *6*, 646.
(10) Kang, S. P.; Chun, M. K.; Lee, H. *Fluid Phase Equilib.* **1998**, *147*, 229.
(11) Anderson, R.; Liamedo, M.; Tohidi, B.; Burgass, W. *J. Phys. Chem. B* **2003**, *107*, 3507.
(12) Ohgaki, K.; Sangawa, H.; Matsubara, T.; Nakano, S. *J. Chem. Eng. Jpn.* **1996**, *29*, 478.
(13) Yezdimer, E. M.; Cummings, P. T.; Chialvo, A. A. *J. Phys. Chem. A* **2002**, *106*, 7982.
(14) Fleyfel, F.; Devlin, J. P. *J. Phys. Chem.* **1988**, *92*, 631.
(15) Fleyfel, F.; Devlin, J. P. *J. Phys. Chem.* **1991**, *95*, 3811.
(16) Sum, A. K.; Burruss, R. C.; Sloan, E. D. *J. Phys. Chem. B* **1997**, *101*, 7371.
(17) Hirai, S.; Okazaki, K.; Kuraoka, S.; Kawamura, K. *Energy Convers. Manage.* **1996**, *37*, 1087.
(18) Udachin, I. A.; Ratchliffe, C. I.; Ripmeester, J. A. *J. Phys. Chem. B* **2001**, *105*, 4200.
(19) Ota, M.; Morohashi, K.; Abe, Y.; Watanabe, M.; Smith, R. L., Jr.; Inomata, H. *Energy Convers. Manage.* **2005**, *46*, 1680.
(20) Ding, L. Y.; Geng, C. Y.; Zhao, Y. H.; Wen, H. *Mol. Simul.* **2007**, *33*, 1005.
(21) Kirchner, M. T.; Boese, R.; Billups, W. E.; Norman, L. R. *J. Am. Chem. Soc.* **2004**, *126*, 9407.
(22) Udachin, K. A.; Ratcliffe, C. I.; Ripmeester, J. A. *J. Supramol. Chem.* **2002**, *2*, 405.
(23) *Materials Studio*, version 4.0; Accelrys Software, Inc.: San Diego, CA, 2006.
(24) Andersen, H. C. *J. Chem. Phys.* **1980**, *72*, 2384.
(25) Berendsen, H. J. C.; Postma, J. P. M.; van Gunsteren, W. F.; DiNola, A.; Haak, J. R. *J. Chem. Phys.* **1984**, *81*, 3684.
(26) Verlet, L. *Phys. Rev.* **1967**, *159*, 98.
(27) IDA, T.; Mizuno, M.; Endo, K. *J. Comput. Chem.* **2002**, *23*, 1071.
(28) Becke, A. D. *J. Chem. Phys.* **1992**, *97*, 9173.
(29) Lee, C.; Yang, W.; Parr, R. G. *Phys. Rev. B* **1988**, *37*, 785.
(30) Khan, A. *J. Chem. Phys.* **1999**, *110*, 11884.
(31) Frisch, M. J.; Trucks, G. W.; Schlegel, H. B.; Scuseria, G. E.; Robb, M. A.; Cheeseman, J. R.; Montgomery, J. A., Jr.; Vreven, T.; Kudin, K. N.; Burant, J. C.; Millam, J. M.; Iyengar, S. S.; Tomasi, J.; Barone, V.; Mennucci, B.; Cossi, M.; Scalmani, G.; Rega, N.; Petersson, G. A.; Nakatsuji, H.; Hada, M.; Ehara, M.; Toyota, K.; Fukuda, R.; Hasegawa, J.; Ishida, M.; Nakajima, T.; Honda, Y.; Kitao, O.; Nakai, H.; Klene, M.; Li, X.; Knox, J. E.; Hratchian, H. P.; Cross, J. B.; Bakken, V.; Adamo, C.; Jaramillo, J.; Gomperts, R.; Stratmann, R. E.; Yazyev, O.; Austin, A. J.;

Cammi, R.; Pomelli, C.; Ochterski, J. W.; Ayala, P. Y.; Morokuma, K.; Voth, G. A.; Salvador, P.; Dannenberg, J. J.; Zakrzewski, V. G.; Dapprich, S.; Daniels, A. D.; Strain, M. C.; Farkas, O.; Malick, D. K.; Rabuck, A. D.; Raghavachari, K.; Foresman, J. B.; Ortiz, J. V.; Cui, Q.; Baboul, A. G.; Clifford, S.; Cioslowski, J.; Stefanov, B. B.; Liu, G.; Liashenko, A.; Piskorz, P.; Komaromi, I.; Martin, R. L.; Fox, D. J.; Keith, T.; Al-Laham, M. A.; Peng, C. Y.; Nanayakkara, A.; Challacombe, M.; Gill, P. M. W; Johnson, B.; Chen, W.; Wong, M. W.; Gonzalez, C.; Pople, J. A. *Gaussian 03*, revision C.02; Gaussian, Inc.: Wallingford, CT, 2004.

(32) Chialvo, A. A.; Housa, M.; Cummings, P. T. *J. Phys. Chem. B* **2002**, *106*, 442.

(33) Hirai, S.; Okazaki, K.; Kuraoka, S.; Kaamura, K. *Energy Convers. Manage.* **1996**, *27*, 1087.

(34) Koh, C. A.; Wisbey, R. P.; Wu, X. P.; Westacott, R. E.; Soper, A. K. *J. Chem. Phys.* **2000**, *113*, 6390.

(35) Demurov, A.; Radhakrishnan, R.; Trout, B. L. *J. Chem. Phys.* **2002**, *116*, 702.

JP811474M